REPORT DOCUMENTATION PAGE		READ INSTRUCTIONS BEFORE COMPLETING FORM
1. REPORT NUMBER NRL Memorandum Report 4356	2. GOVT ACCESSION NO. AD -AC90524	3. RECIPIENT'S CATALOG NUMBER
4. TITLE (and Subtitle) PREHEAT STUDIES ON LASER ABLATIVELY-ACCELERATED FOILS		5. TYPE OF REPORT & PERIOD COVERED Interim report on a continuing NRL problem.
		6. PERFORMING ORG. REPORT NUMBER
7. AUTHOR(s) E. A. McLean, S. H. Gold, J. A. Stamper, R. R. Whitlock, H. R. Griem, S. P. Obenschain, B. H. Ripin, S. E. Bodner, and M. J. Herbst*		8. CONTRACT OR GRANT NUMBER(s)
9. PERFORMING ORGANIZATION NAME AND ADDRESS Naval Research Laboratory Washington, DC 20375		10. PROGRAM ELEMENT, PROJECT, TASK AREA & WORK UNIT NUMBERS 67-0859-A-0
11. CONTROLLING OFFICE NAME AND ADDRESS U. S. Department of Energy Washington, DC 20545		12. REPORT DATE October 13, 1980
		13. NUMBER OF PAGES 17
14. MONITORING AGENCY NAME & ADDRESS(if different from Controlling Office)		15. SECURITY CLASS. (of this report) UNCLASSIFIED
		15a. DECLASSIFICATION/DOWNGRADING SCHEDULE

16. DISTRIBUTION STATEMENT (of this Report)

Approved for public release; distribution unlimited.

17. DISTRIBUTION STATEMENT (of the abstract entered in Block 20, if different from Report)

19. KEY WORDS (Continue on reverse side if necessary and identify by block number)

20. ABSTRACT (Continue on reverse side if necessary and identify by block number)

The achievement of laser fusion requires the inward acceleration of pellet shells to very high velocity without excessive preheat of the pellet fuel. In a study of ablatively accelerated thin planar Al foils, we have determined the complete time history of the rear surface temperatures, and evaluated the energy transport mechanisms that contribute to the heating. Extrapolation to larger, reactor-sized pellets indicates that preheat is minimal at low laser irradiances.

DD FORM 1473 EDITION OF 1 NOV 65 IS OBSOLETE
S/N 0102-LF-014-6601

i

5

PREHEAT STUDIES ON LASER ABLATIVELY-ACCELERATED FOILS

In current laser fusion studies, it is recognized that preheat
of the target fuel of more than a few electron volts can significantly
reduce the degree of compression and pellet yield that can be achieved.[1]
Therefore, it is of considerable importance to know the temperature on
the inside of the target shell. Such knowledge will allow one to choose
the proper isentrope for compression calculations as well as to check the
predictions of detailed numerical simulations of laser driven implosions.
Using laser-driven ablation we have accelerated thin planar foils, which
simulate the early behavior of an imploding pellet shell, to velocities
of 1.5×10^7 cm/sec for CH targets and 3×10^6 cm/sec for Al targets.[2]
Here we report measurements of rear surface temperatures of accelerated Al
targets which remain below 3 eV through the bulk of the laser pulse, achieving
a directed kinetic energy per particle greater than 80 times the temperature.
The temperatures are inferred by measuring the absolute rear surface
continuum emission with monochromators and then using blackbody emission
assumptions, which we verify.[3] These are the first time-resolved temperature
measurements for these conditions. Similar techniques have been used
elsewhere to measure temperatures and velocities associated with high-
pressure shock phenomena.[4,5]

The experiments were performed using one beam of the NRL Pharos II
Nd:phosphate-glass laser system (1.05 μm) with up to 200 joules on target
in a 4-nsec FWHM pulse. Irradiation uniformity is improved and edge
effects are minimized by using large focal spot diameters (typically 1 mm)
obtained by placing the target off-focus toward the laser to produce
irradiances of $1-6 \times 10^{12}$ W/cm^2. Temperature measurements were made on
Al foil targets ranging in thickness from 4-23 μm. The experimental

setup is shown in Fig. 1. Two 3/4-m-monochromators equipped with 1-nsec rise time photomultipliers[6] measure continuum intensity from the rear surface of the target at two wavelengths simultaneously. Using a beam splitter, both monochromators make observations along a common axis positioned 6 degrees off the laser axis (but normal to the target axis). Good shot-to-shot reproducibility allows a parameter study in target thickness, target material, and wavelength of observation. The demagnified image of the spectrograph slit (see Fig. 1, inset), samples a central portion of the focal spot area. Typically, the slit widths are set to observe a 17-33 $\overset{o}{A}$ bandwidth. An absolute calibration of the optics, the spectrographs, and the photomultipliers is made "in situ" using a tungsten ribbon-filament lamp, calibrated by the National Bureau of Standards.[7]

A survey over the spectral range 3500-6500 $\overset{o}{A}$ was made by taking time-integrated spectra both parallel and perpendicular to the rear target surface. The continuum wavelength intervals were chosen at positions where no spectral lines were observed. Several experiments were done to check the assumption that the rear surface radiates as a blackbody. Figure 2 shows peak intensity versus wavelength data for Al foils of 4 μm, 7 μm, and 12 μm thickness. This figure demonstrates the magnitude of shot-to-shot scatter and calibration errors. It is seen that the intensity data have the magnitude and approximate wavelength dependence expected from a blackbody.

In addition, the peak intensity of a strong aluminum spectral line was found to be the same (+20%) as the neighboring continuum. This would be the case if the radiation was coming from an isothermal, optically-thick plasma, i.e., a blackbody. We conclude that the blackbody assumptions are justified.

LASER
BEAM
$\lambda = 1.05\mu m$

TARGET
CHAMBER

6°

LENS

6.3°

IR BLOCKING
FILTER

BEAM SPLITTER

MONOCHROMATOR

MONOCHROMATOR

FAST PHOTOMULTIPLIERS

|—1 mm—|

LASER
FOCAL
SPOT

SLIT IMAGE

Fig. 1 — Experimental setup showing collection optics and field of view of
monochromators.
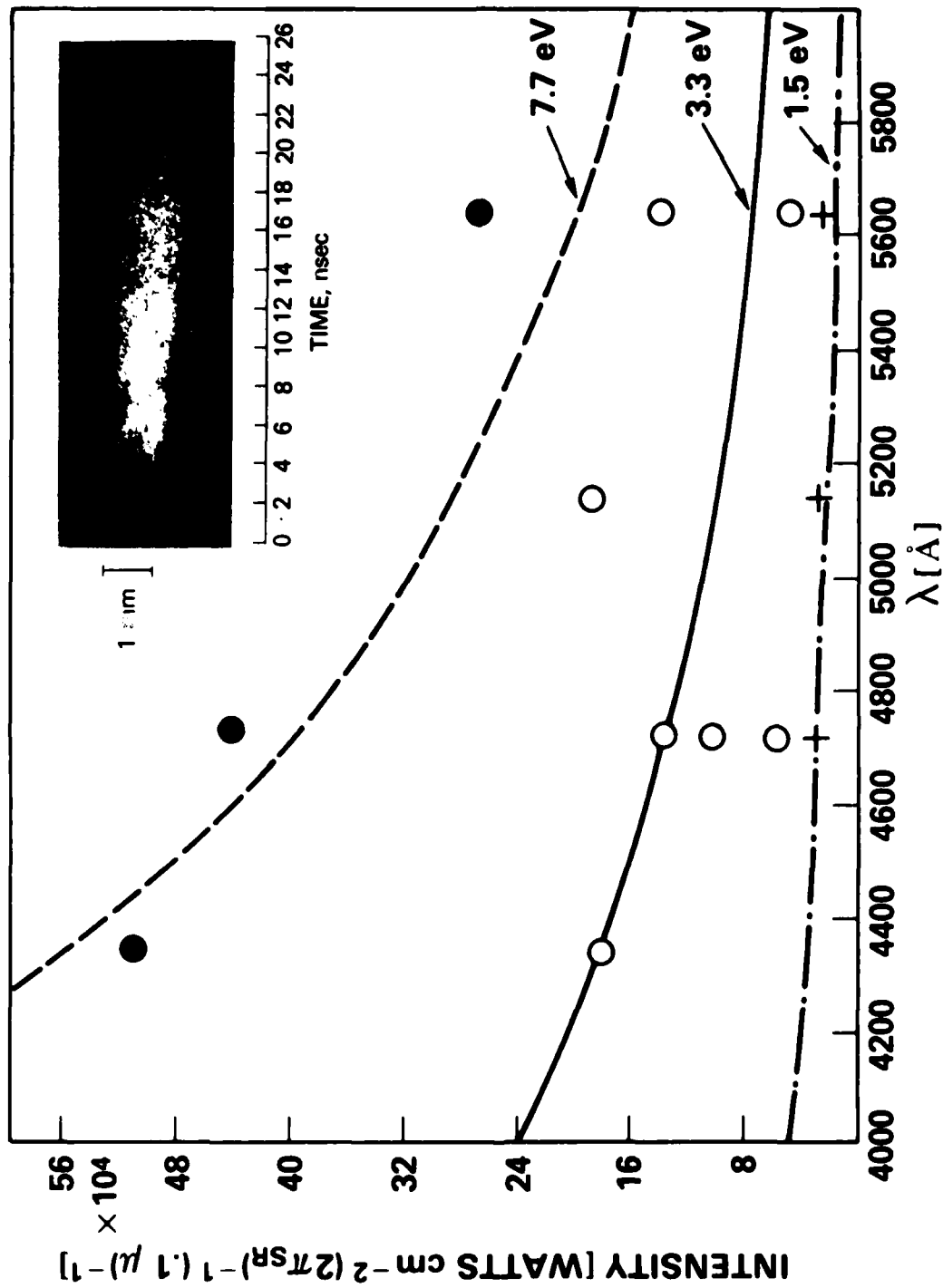
Fig. 2 — Rear surface continuum intensity vs. wavelength for 3 Al foil thicknesses at 5×10^{12} W/cm^2. Curves are black-body intensities at the given temperatures. (Data points: ● = 4µm Al ; o = 7µm Al; + = 12µm Al). Inset shows streak photograph of rear surface luminosity across a diameter of the focal spot.

4

Interferometric plasma density measurements on the rear surface of the accelerated target obtained with a laser (5270 $\overset{o}{A}$) probe beam passing tangentially to the target surface gave maximum densities of approximately 10^{19} cm^{-3} and a gradient scalelength of 50 μm at the visible rear surface. However, these density measurements are limited by the opacity of the 1 mm plasma path length for the probe light, and by refraction of the probe light out of the f/2 collection optics due to a steep electron density gradient. Opacity calculations[8] show that, at the emission wavelengths observed and at a temperature of 0.5-2 eV, the plasma has an opacity of about 1 for a density of several times 10^{20} cm^{-3} and a path length of 10 microns. Therefore, the temperature we are measuring characterizes a region in the density interval 5×10^{19} cm$^{-3} < n < 5 \times 10^{20}$ cm^{-3}. (An optical probe beam directed perpendicularly at the rear side of the target was found to be strongly absorbed when the temperature reached a few tenths of an electron volt.)

Figure 3 shows the time history of the rear surface temperatures for Al foil targets of several different thicknesses. Accuracy of the temperature determination is better than a factor of 2 for $T > 2$ eV and improves to $\pm 20\%$ at $T_e = 0.4$ eV. In each case, heating occurs during the period of the laser pulse but the temperature continues to increase for several nanoseconds thereafter. The peak temperatures are seen to shift to later times and lower values as the target thickness increases. Figure 3(inset) shows the dependence of temperature on target thickness just after the acceleration (which is over by about +2 to+3 nsec). Additionally, the peak rear surface temperature was found to increase linearly with increasing irradiance (or energy) over the irradiance range $2 - 6 \times 10^{12}$ W/cm^2. The peak temperature (T_e) for Al as well as CH and C foils, all fit a single

hyperbola, $T_e \, \rho_A = 8 \times 10^{-3}$ eV gm cm^{-2} at 5×10^{12} W/cm^2, where the areal density ρ_A is the product of material density and target thickness. The peak temperatures ranged from 34 eV for a 2.5 μm CH foil to 0.8 eV for 23 μm Al foil.

Possible mechanisms for energy transport to the rear of targets include fast electrons, x rays, thermal conduction and shocks. The contributions of these phenomena have been evaluated by separate measurements and by considerations of the time history and parametric behavior of the measured temperature.

First, the lack of measurable x-ray emission (0.1 erg) in the energy range 20-50 keV, (corresponding to radiation from electrons with ranges comparable to target thickness) from the front side of the foils[9] demonstrates that there is insufficient fast electron energy (5×10^{-5} J) to cause appreciable heating of the rear target surface.

Second, time-resolved studies have shown that the x-ray emission (>1 keV) very closely follows the time history of the incident laser irradiance, so that x-ray preheat effects should closely follow the time-integrated laser pulse (Fig. 3). Based on the known range and measured intensities of x rays in the energy range of 1.5 - 50 keV emitted from the front side of Al targets, the important x rays for the purpose of preheating the rear target surface are the x-ray line and continuum radiation between 1.6 and 2.3 keV. (The much lower intensity continuum emission just below the K-edge at 1.56 keV, as yet unresolved, may also be an important preheat agent.) The time-integrated x-ray line spectrum was measured on an absolute basis (to an estimated accuracy of a factor of 2) and the x-ray energy deposited throughout the target was calculated, assuming spatial uniformity of the x-ray source and using cold material absorption coefficients. A knowledge of the equation

6

of state is necessary in order to convert preheat energy deposition to temperature. We assume the target foil material remains near solid density for the times of interest, and use tabulated heat capacity data[10] to determine the temperature resulting from the calculated local x-ray deposition (curve at 3 nsec, Fig. 4). We find that the rear-side temperature rise during the laser pulse is consistent with 1.6 - 2.3 keV x-ray deposition.

Third, using formulae and tabulated data for thermal conduction and radiative diffusion[10] and the tabulated data for heat capacities, numerical calculations assuming a fixed temperature at a point 1 μm in from the front surface and no losses from the rear surface (curves at 6 and 12 nsec, Fig. 4) show that thermal conduction may explain the upward drift in temperature after termination of the laser pulse.

Fourth, the contribution to the heating of the target due to shock waves that may be present is difficult to evaluate precisely. From measurement of ablation particle velocities, as well as gross acceleration of the target foil, we infer a peak ablation pressure of ~2 Mbar at 5×10^{12} W/cm^2 on Al. A single 2 Mbar shock propagating into cold Al will produce a 75% density increase, a 0.8 eV temperature rise, and a shock velocity of 1.3×10^{6} cm/sec.[10] In fact, the small early temperature rise for the thicker Al targets (12-23 μm) appears consistent with such a model. For thin targets, however, one must use a hydrodynamic code to evaluate the magnitude of shock wave heating; multiple reflections occur because the rise time of the pressure pulse is longer than the shock transit time through the target. Two different hydrodynamic codes, which have been run for our experimental conditions, indicate that the x-ray deposition is the major contributor to the rear surface heating for 4-12 μm Al targets.[11,12] The codes agree within a factor of two with the observed temperature and closely match the temporal behavior for these targets.

7
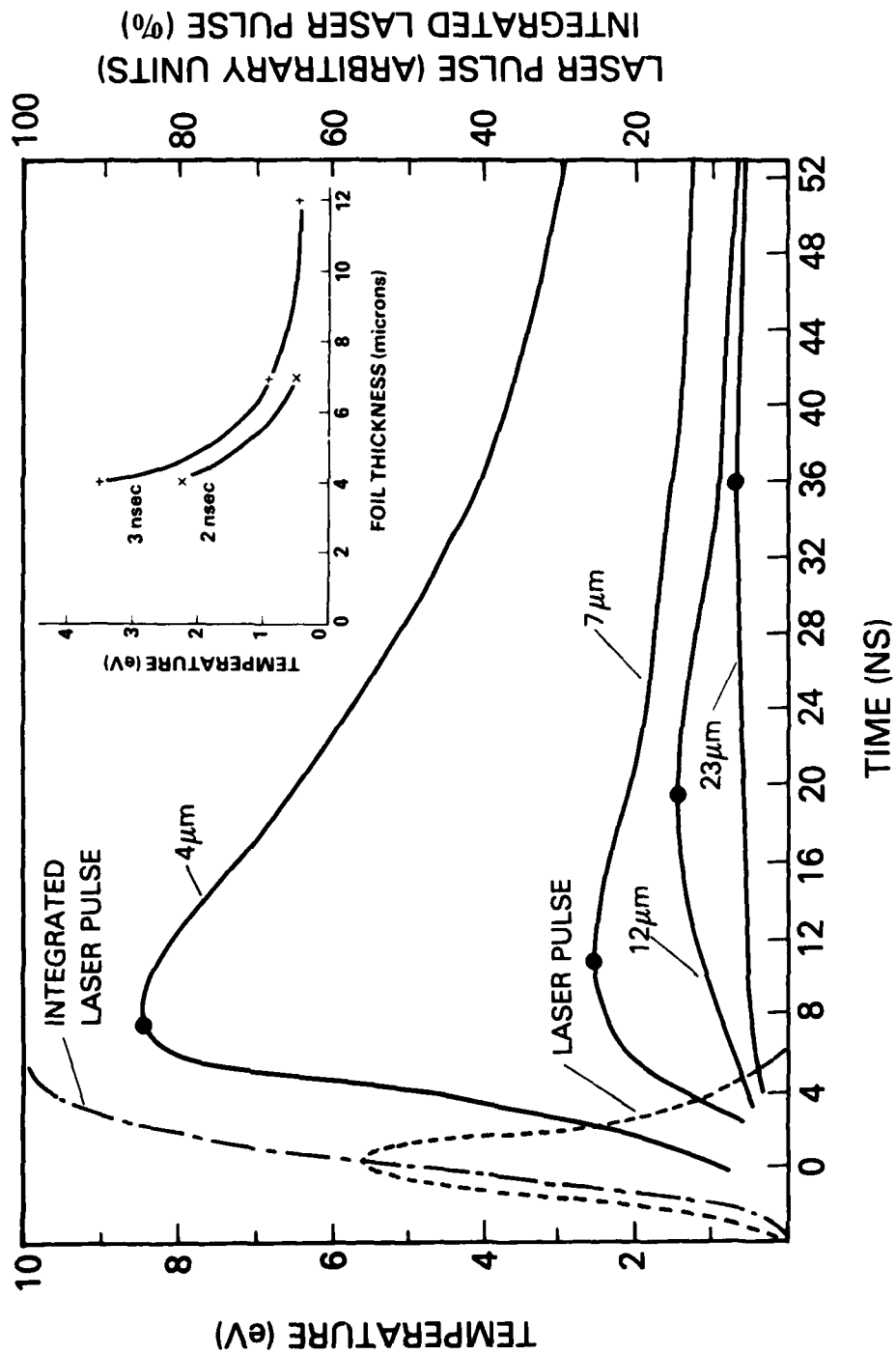
Fig. 3 — Rear surface temperature vs. time for 4 Al foil thicknesses at 5 x 10^12 W/cm^2, 1 mm spot, λ = 4717 Å, Δλ = 33Å. Dotted curve is the time history of the laser pulse and the dashed curve is the integrated laser pulse. The time t = 0 corresponds to the time of the peak of the laser pulse. Inset shows rear surface temperature vs. Al foil thickness at two times at the end of the acceleration process.
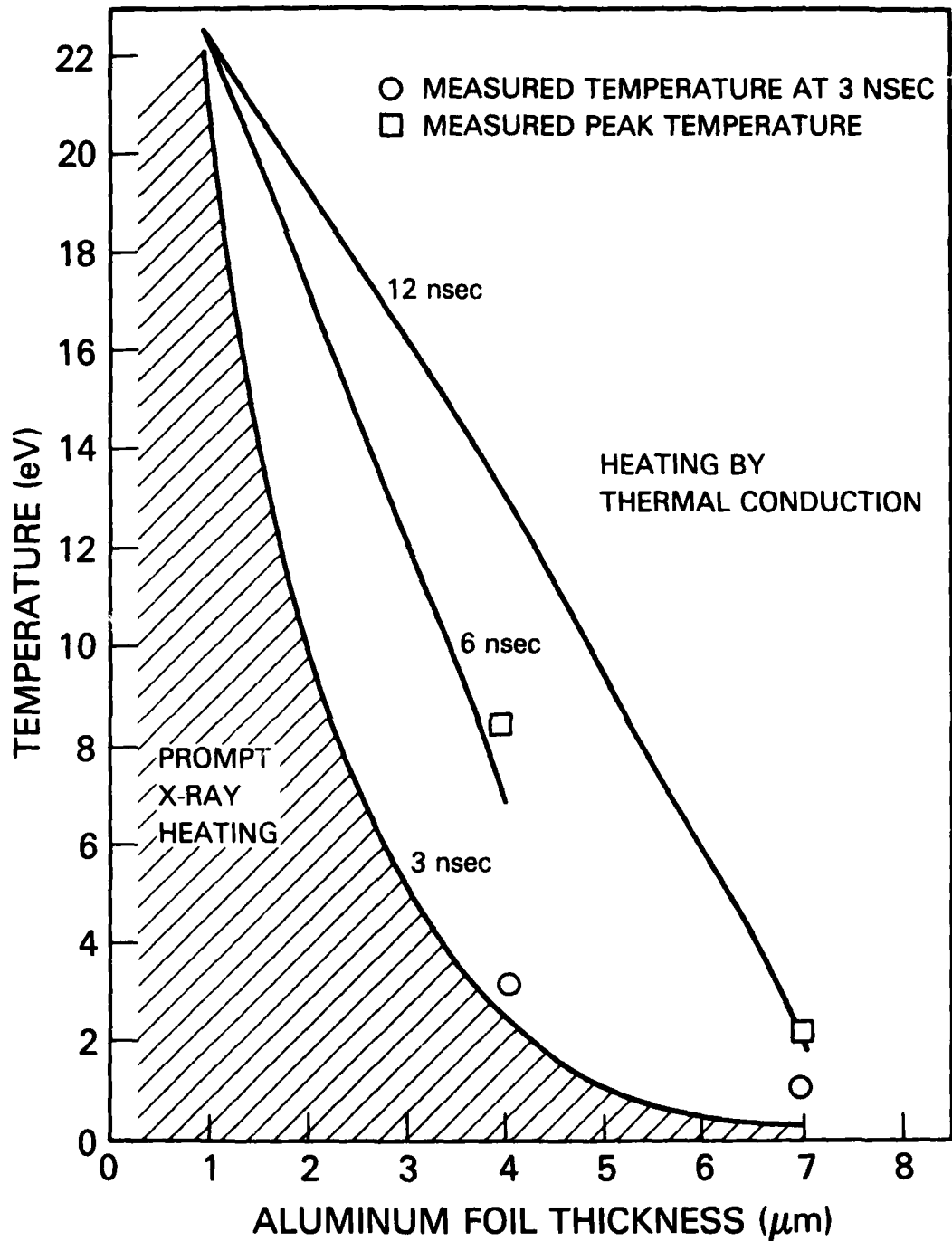
Fig. 4 — Rear surface temperature vs. Al foil thickness showing the prompt x-ray heating at 3 nsec, and prompt plus thermal conduction heating at 6 nsec for the 4 μm foil and at 12 nsec for the 7 μm foil. The square data points are measured temperature values at 6 nsec for the 4 μm Al foil and at 12 nsec for the 7 μm Al foil.

The late time heating and cooling of the rear surface can be understood in terms of an energy transport balance into and out of the rear surface. Thermal conduction calculations similar to those previously mentioned suggest that ordinary axial thermal conduction can account for the slow upward drift of the rear surface temperature that is seen on the thicker targets. The importance of lateral thermal conductivity on the late time development of the rear surface temperature is indicated by measurements on a 7- μm-thick Al foil. These show that when the focal spot size is reduced from 1 mm to ¼ mm diameter at constant irradiance, the peak temperature is lower by 50% and occurs earlier in time, and the temperature decays more rapidly.

We have examined the possibility of energy flowing around our target foil, which has been reported on disc targets with higher irradiance CO_2 lasers.[13] By increasing the width of the foil from 3 mm to 1 cm, we see less than 10% change in the rear surface temperature, and conclude that the effect of energy flowing around the target, if present, is small. There is also the possibility of energy flowing around the edges of the slug of accelerated material ("cookie-cutter" model).[14] Streak photography of the rear surface visible emission (Fig. 2, inset), as well as time-integrated photography, show no sign of either of these effects.

In conclusion, we have measured the time history of the rear surface temperature of foils accelerated by laser ablation. The relative effects of x rays, shocks, thermal conduction, and fast electrons upon preheating this surface have been evaluated. It is concluded that for our conditions direct heating by soft x rays followed by thermal conduction appears capable of explaining most of the heating observed in thinner foils. Shock waves

10

are more important for the thicker targets. The energy flows through rather than around the targets, providing a close analogy to the laser ablative implosion of pellet shells.

It should be noted that in these experiments the rear surface temperature of even the thinnest Al targets (4 μm) remain on a low isentrope ($\leqslant$3 eV) throughout the acceleration process. Proposed low-irradiance, reactor-sized pellets[15] would have thicker shells ($\geqslant$ 50 μm) and thus even less heating by x rays and thermal conduction.

REFERENCES

1. J. Nuckolls, L. Wood, A. Thiessen, G. Zimmerman, Nature, 239, 139 (1972).

2. R. Decoste, S.E. Bodner, B.H. Ripin, E.A. McLean, S.P. Obenschain, and C.M. Armstrong, Phys. Rev. Lett. 42, 1673 (1979).

3. E.A. McLean, S.P. Obenschain, J.A. Stamper, S.H. Gold, B.H. Ripin, R. Decoste, and S.E. Bodner, Conference Record - 1979 IEEE International Conference on Plasma Science, June 4-6, 1979, Paper 3A8.

4. L.R. Veeser and J.C. Solem, Phys. Rev. Lett. 40, 1391 (1978); and R.J. Trainor, J.W. Shaner, J.M. Auerbach, and N.C. Holmes, Phys. Rev. Lett. 42, 1154 (1979).

5. P.A. Urtiew, UCRL Report No. UCRL-51432, 1973 (unpublished); and G.A. Lyzenga and T.J. Ahrens, Rev. Sci. Instrum. 50, 1421 (1979).

6. G. Beck, Rev. Sci. Instrum. 47, 537 (1976).

7. C.R. Barber, J. Sci. Inst. 23, 238 (1946).

8. Norman H. Magee, Jr. of Los Alamos Scientific Laboratory has kindly provided us with opacity calculations for aluminum.

9. F.C. Young, private communication.

10. S.L. Thompson and H.S. Lauson, Sandia Laboratories Report Nos. SC-RR-710713 and SC-RR-710714 (unpublished).

11. S.J. Gitomer, to be published.

12. M.K. Matzen, private communication.

13. N.A. Ebrahim, C. Joshi, D.M. Villeneuve, N.H. Burnett, and M.C. Richardson, Phys. Rev. Lett. 43, 1995 (1979).

14. R.E. Morse, et al., to be published.

15. Yu. V. Afanas'ev et al. Pis'ma Zh. Eksp. Teor. Fiz. $\underline{21}$, 150 (1975) [JETP Lett. $\underline{21}$, 68 (1975)].

DISTRIBUTION LIST

USDOE (50 copies)
P.O. Box 62
Oak Ridge, TN 37830

National Technical Information Service (24 copies)
U.S. Department of Commerce
5285 Port Royal Road
Springfield, VA 22161

Los Alamos Scientific Laboratory
Los Alamos, NM 87545
Attn: Dr. R. Godwin
      Dr. S. Gitomer
      Dr. J. Kindel

NRL, Code 2628 (35 copies)

NRL, Code 4730 (100 copies)

NRL, Code 4700 (25 copies)

University of Rochester
Rochester, NY 14627
Laboratory for Laser Energetics
Attn: Dr. J. Soures
      Dr. W. Seka

USDOE (6 copies)
Office of Inertial Fusion
Washington, D.C.
Attn: Dr. G. Canavan
      Dr. R. Schriever
      Dr. S. Kahalas
      Dr. T. Godlove
      Dr. K. Gilbert

KMS Fusion
3941 Research Park Drive
P.O. Box 1567
Ann Arbor, MI 48106
Attn: Dr. F. Mayer

Lawrence Livermore Laboratory
P.O. Box 808
Livermore, CA 94551
Attn: Dr. D. Attwood, L481
      Dr. W. Kruer, L545
      Dr. J. Lindl, L32
      Dr. C. Max, L545
      Dr. A. Glass
      Dr. L. Coleman
      Dr. J. Nuckolls
      Dr. W. Mead
      Dr. N. Ceglio
      Dr. R. Kidder

Institut fur Plasmaphysik
8046 Garching
Bei Munchen
West Germany
Attn: Dr. R. Sigel

National Research Council
Division of Physics
100 Susser Drive
Ottawa K1A-OR6, Canada
Attn: Dr. J. Alcock

University of Quebec
INRS Energie
Case Postale 1020
Varennes, Quebec
Attn: Dr. T. Johnston
      Dr. R. Decoste

INTERNAL DISTRIBUTION

Code 4790   Dr. D. Colombant
            Dr. W. Manheimer

Department of Physics and Astronomy
University of Maryland
College Park, MD 20740
Attn: Dr. H. Griem

Rutherford Laboratory
Chilton, Didcot
Oxon OX11OQX
England
Attn: Dr. M. Key
      Dr. T. Raven

15

Sandia Laboratory
Albuquerque, NM
Attn: Dr. K. Matzen
     Dr. J. Anthes
     Dr. R. Palmer

Institute for Laser Engineering
Osaka University
Suita Osaka, 565
Japan
Attn Dr. C. Yamanaka

Shanghai Institute of Optics and Fine Mechanics
Academia Sinica
Shanghai, PRC
Attn: Prof. Gan Fu-xi
     Prof. Yu Wen-yan
     Prof. Xu Zhi-zhan
     Prof. Deng Xi-ming
     Prof. Tan Wei-han
     Mr. Pan Cheng-min

Soreq Nuclear Center
Yavne, Israel
Attn: Dr. A. Krumbein

INTERNAL DISTRIBUTION

Code 4040 J. Boris
           J. Gardener
           J. Orens

Dr. James Lunney
Dept. of Pure and Applied Physics
Queens University
Belfast, N. Ireland

Defense Technical Information Center
Cameron Station
5010 Duke Street
Alexandria, VA 22314